Case Studies in Thermal Engineering 53 (2024) 103793

Contents lists available at ScienceDirect

Case Studies in Thermal Engineering

journal homepage: www.elsevier.com/locate/csite

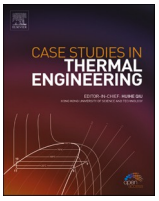

Comprehensive performance assessment on LBE-helium heat exchangers for the ADS based on extension theory

Keyong Cheng [a,b,c,*], Zhijiang Meng [a,d], Xunfeng Li [a,b,d], Junlin Chen [a,b], Xiulan Huai [a,b,d]

[a] Institute of Engineering Thermophysics, Chinese Academy of Sciences, Beijing, 100190, China
[b] Nanjing Institute of Future Energy System, Nanjing, 210000, China
[c] University of Chinese Academy of Sciences, Nanjing, 211135, China
[d] School of Engineering Science, University of Chinese Academy of Sciences, Beijing, 101408, China

ARTICLE INFO

Handling Editor: Huihe Qiu

Keywords:
Extension theory
Heat exchanger
Performance evaluation
Shell-and-tube heat exchangers
Printed circuit heat exchangers
Accelerator driven sub-critical system

ABSTRACT

Researches about comprehensive, systemic and multi-level assessment methods are limit. Therefore, a comprehensive assessment method of heat exchangers based on extension theory is proposed. Heat transfer, pressure drop, mechanism, safety and reliability, economy, structure, mechanism and production performance are considered and evaluated in detail. By using this method, the comprehensive performances of the shell-tube and printed circuit heat exchangers as the intermediate heat exchanger of the accelerator driven sub-critical system are evaluated for comparison. The results show that the economy performance and pressure drop for the shell-tube heat exchanger attain the highest grades because the processing technology is mature and flow velocity is lower. However, the structure performance parameter is the lowest level due to its large volume and mass. For the printed circuit heat exchanger, the safety and reliability performance attains the lowest grade due to its easily blocked mini-channels and the manufactured thin plate. However, the mechanism performance shows the highest grade. In addition, the pressure drop performance also attains the highest grade due to its large cross-sectional area and low flow velocity. In conclusion, the comprehensive performance of the printed circuit heat exchanger is theoretically better than the shell-tube heat exchanger.

1. Introduction

As a clean and renewable source of energy, nuclear energy has the unique advantage and development potential on reducing the emissions of greenhouse gases and mitigating the pressure of energy transmission effectively [1,2]. Currently, how to dispose the nuclear waste has the constraint on the development of nuclear energy. Through the collision of proton beam generated by the accelerator with the spallation target of lead-bismuth eutectic (LBE), the accelerator driven sub-critical system (ADS) could drive and sustain the process of the nuclear transmutation, and reduce the life and radioactive property of nuclear wastes, and therefore is one of the effective resolutions [3]. In this system, LBE is adopted as not only the medium of the spallation target but also the coolant of the reactor due to its good thermal-physical properties [4–6]. The heat produced by the reactor is transferred from LBE to the working fluid of the power generating system through the intermediate heat exchanger (IHE), and the performance of the IHE plays significant impacts on the functions of the ADS and the power generating system. Therefore, systematic and reasonable performance evaluation

* Corresponding author. Institute of Engineering Thermophysics, Chinese Academy of Sciences, Beijing, 100190, China.
E-mail address: chengkeyong@iet.cn (K. Cheng).

https://doi.org/10.1016/j.csite.2023.103793
Received 19 May 2023; Received in revised form 19 October 2023; Accepted 18 November 2023
Available online 28 November 2023
2214-157X/© 2023 The Authors. Published by Elsevier Ltd. This is an open access article under the CC BY-NC-ND license (http://creativecommons.org/licenses/by-nc-nd/4.0/).

on the IHE is of great significance.

At first, the performance assessment on the IHE with LBE is from the first principle of thermodynamics. Heat transfer rate, heat transfer coefficient and pressure drop are directly adopted to present heat transfer and flow characteristics of heat exchangers. For example, Ma et al. [7] experimentally investigated the effect of the straight and U-type tubes on the performance of the IHE with LBE. The heat transfer coefficients and pressure drops are compared between these two heat exchangers. Xi et al. [8] experimentally tested the performance of a shell-and-tube heat exchanger (STHE) with LBE and helium. The heat transfer rate, the overall heat transfer coefficient and pressure drop of the heat exchanger are obtained with increasing the Reynolds number and inlet temperature. In order to increase commonality, parts of research investigate the dimensionless performance parameters related to heat exchangers, such as Nusselt number, friction factor, effectiveness and number of transfer units (NTU). Chen et al. [9] numerically simulated a STHE with LBE and they utilized the overall heat transfer coefficient to compute the NTU and effectiveness of the heat exchanger for evaluation. Wang et al. [10] compared the effectiveness and friction factor of the STHE with LBE and helium with those concluded from correlations. Khan et al. [11] designed a compact heat exchanger with LBE and the heat transfer coefficient and Nusselt number are adopted to evaluate the performance of the heat exchanger. In order to fully consider the flow and heat transfer characteristics of the IHE, a comprehensive performance evaluation criterion (PEC) is introduced. Zhao et al. [12] changed straight tubes with twisted tubes for the IHE. The results show that the PEC of the twist-tube heat exchanger is improved by 1.2–1.7 times compared with the straight-tube one. Yang et al. [13] numerically studied the STHE with LBE and water, and the PEC is analyzed to optimize the inlet velocity of LBE.

In recent years, with the development of manufacturing technology, the printed circuit heat exchanger (PCHE) has been chosen as the IHE for the nuclear power generation system because of its high efficiency, compactness, reliable, and easy to manufacture [14–18]. Wang et al. [19] investigated the performance of the PCHE with LBE and helium. The heat transfer coefficient, Nusselt number, pressure drop and PEC are adopted to evaluate three different designs. Xu et al. [20] chose Nusselt number, friction factor, and PEC to study the performance of the PCHE with LBE and supercritical CO_2.

In order to consider the irreversible loss during the heat transfer process, Wang et al. [21] analyzed the IHE with LBE and helium from the secondary principle of thermodynamics, and exergy efficiency is obtained under different inlet temperatures and mass flow rates of LBE, and exergy loss and entropy generation referring to temperature difference and pressure drop are obtained. To study the irreversibility of the convective heat transfer characteristics of LBE, Zhang et al. [22] introduced an evaluation criterion E_p which is the ratio of Nusselt number and global dimensionless entropy generation.

Based on the above research, it is concluded that currently the evaluation of the IHE with LBE mainly focus on the performance of flow and heat transfer characteristics. As a matter of fact, during the applications many other performances of the heat exchangers are equally important, such as mechanical performance, structural performance, safety and reliability performance, economic performance and production cycle [23–28]. However, according to authors' knowledge, so far there has been no research considering all these performances of the IHE with LBE systematically. Therefore, in order to reasonably assess the performance of the IHE for the ADS, a comprehensive evaluation method of heat exchangers is proposed based on extension theory in this paper, which includes eighteen parameters. The STHE and the PCHE are adopted as the IHE for comparison. Through building the matter element model and calculating correlated functions, performance parameters of the STHE and the PCHE in the index and criterion layers are obtained. Based on these data, the comprehensive performance of the STHE and the PCHE are concluded by calculated the characteristics value.

2. Comprehensive performance assessment method

2.1. Construction of assessment system

Extension theory and method is to study matter element and its transformation [29]. The matter element is the logical cell for the extension model and organically combines the quality and quantity of things. This method has been applied in the fields of management and decision, artificial intelligence and computer, and control and detection [30–33]. In this study, extension theory and

Table 1
Evaluation system of heat exchanger.

Target layer	Criterion layer	Index layer
Comprehensive performance of heat exchanger	Heat transfer	Heat transfer area
		Average temperature difference
		Heat transfer coefficient
	Pressure drop	Fluid velocity
		Pressure loss
	Mechanism	Allowable stress
		Design pressure
		Weld joint factor
	Safety and reliability	Lost circulation resistance
		Corrosion resistance
		Anti-fouling
	Economy	Manufacture and installation cost
		Depreciation cost
		Maintenance cost
	Structure	Volume mass
	Production	Design cycle
		Processing cycle

method is adopted to assess the performance of heat exchangers. The matter element model for the multi-level comprehensive extension evaluation of heat exchangers is built, which transfers the quantitative description of the evaluation index to the quantity description.

Multiple parameters for the evaluation of the heat exchangers are needed to be considered because the performance of the heat exchanger is affected by various factors, and these factors are both interrelated and mutually constraining. Therefore, considering the rigor, practicality, and operability of the evaluation method and scientific and independent evaluation index, the evaluation system of the heat exchanger consists of three layers: target layer, criterion layer and index layer. Seven parameters are summarized in the criterion layer and eighteen parameters in the index layer, which is shown in Table 1 [34]. It is noteworthy that this evaluation system is the collection of dynamic indexes and could be supplemented and adjusted according to the experience of decision makers, the actual situation of craft production, special requirement of operating conditions and the need of different users.

2.2. Matter element model

For the multi-level comprehensive performance evaluation system of the heat exchanger, the m-dimensional first-level matter element model S_0 is shown as follows:

$$S_0 = \begin{bmatrix} T_0 & a_1 & b_1 \\ & a_2 & b_2 \\ & \vdots & \vdots \\ & a_m & b_m \end{bmatrix} \tag{1}$$

in which T_0 stands for the specific scheme in the target layer of the heat exchanger; a_i ($i = 1, 2, \ldots, m$) stands for the criterion in the first-level model; b_i is the value of T_0 relating to a_i.

The n-dimensional second-level matter element model S'_0 is shown as follows:

$$S'_0 = \begin{bmatrix} T_{0h} & a_{h1} & b_{h1} \\ & a_{h2} & b_{h2} \\ & \vdots & \vdots \\ & a_{hn} & b_{hn} \end{bmatrix} \tag{2}$$

in which T_{0h} ($h = 1, 2, \ldots, m$) stands for the criterion in the criterion layer; a_{hk} ($k = 1, 2, \ldots, n$) stands for the index in the second-level model; b_{hk} is the value of T_{0h} relating to a_{hk}.

2.3. Classical and joint domains

Based on the related standards of heat exchangers, accumulated database and expert opinions, each index in this evaluation system is divided into four grades ($p = 4$): poor, medium, good and excellent (from 1 to 4). Therefore, the m-dimensional first-level matter element model S_0 relating to evaluation grade j ($j = 1, 2, \ldots, p$) is expressed as:

$$S_0 = \begin{bmatrix} T_{0j} & a_1 & R_{0j1} \\ & a_2 & R_{0j2} \\ & \vdots & \vdots \\ & a_m & R_{0jm} \end{bmatrix} = \begin{bmatrix} T_{0j} & a_1 & (x_{0j1}, y_{0j1}) \\ & a_2 & (x_{0j2}, y_{0j2}) \\ & \vdots & \vdots \\ & a_m & (x_{0jm}, y_{0jm}) \end{bmatrix} \tag{3}$$

in which T_{0j} is evaluation grade in the target layer. Classical domain R_{0ji} is the value range of evaluation grade T_{0j} relating to a_i.

The m-dimensional first-level matter element model relating to all the evaluation grades S_p is expressed as:

$$S_p = \begin{bmatrix} T_p & a_1 & R_{p1} \\ & a_2 & R_{p2} \\ & \vdots & \vdots \\ & a_m & R_{pm} \end{bmatrix} = \begin{bmatrix} T_p & a_1 & (x_{p1}, y_{p1}) \\ & a_2 & (x_{p2}, y_{p2}) \\ & \vdots & \vdots \\ & a_m & (x_{pm}, y_{pm}) \end{bmatrix} \tag{4}$$

in which T_p stands for all the evaluation grades in the target layer. Joint domain R_{pi} is the value range of all the evaluation grades T_p relating to a_i.

Similarly, the n-dimensional second-level matter element model relating to the evaluation grade could be deduced in the same way, and so are the classical and joint domains.

2.4. Weight

In this study, the weights of the performance indexes of the heat exchanger are set based on fuzzy analytic hierarchy process [34, 35]. First, the basic idea of this method is to rank the affiliation of various factors in the evaluation system of the heat exchanger into several levels from high to low, and build the correlation of the factors in different layers. Then, based on the judgment of certain objective fact, mathematical methods are used to determine order weight of all the elements at each level according to the relative importance. At last, the problem is analyzed and solved through the ranking results.

The weight of the parameter in the criterion layer w_i is shown as follows:

$$\sum_{i=1}^{m} w_i = 1 \tag{5}$$

The weight of the parameter in the index layer w_{hk} is shown as follows:

$$\sum_{k=1}^{n} w_{hk} = 1 \tag{6}$$

2.5. Correlated function and evaluation grade

The correlated function F of the m-dimensional first-level matter element model relating to evaluation grade j for the comprehensive performance assessment system of the heat exchanger is expressed as:

$$F_j(b_i) = \begin{cases} \dfrac{\xi(b_i, R_{0ji})}{K(b_i, R_{0ji}, R_{pi})\left|R_{0ji}\right|}, b_i \in R_{0ji} \\ \dfrac{\xi(b_i, R_{0ji})}{K(b_i, R_{0ji}, R_{pi})}, b_i \notin R_{0ji} \end{cases} \tag{7}$$

$$\xi(b_i, R_{0ji}) = \left|b_i - (x_{0ji} + y_{0ji})/2\right| - (y_{0ji} - x_{0ji})/2 \tag{8}$$

$$\xi(b_i, R_{pi}) = \left|b_i - (x_{pi} + y_{pi})/2\right| - (y_{pi} - x_{pi})/2 \tag{9}$$

in which $\xi(b_i, R_{0ji})$ is the distance between point b_i and internal R_{0ji} at evaluation grade j. $\xi(b_i, R_{pi})$ is the distance between point b_i and internal R_{pi}.

$K(b_i, R_{0ji}, R_{pi})$ is the location of point b_i compared to internal R_{0ji} and R_{pi}, and could be expressed as:

$$K(b_i, R_{0ji}, R_{pi}) = \begin{cases} \xi(b_i, R_{pi}) - \xi(b_i, R_{0ji}), b_i \in R_{0ji} \\ -1, b_i \notin R_{0ji} \end{cases} \tag{10}$$

The relation of comprehensive evaluation with the evaluation grade F' could be expressed as:

$$F_j'(b_i) = \sum_{i=1}^{m} w_i F_j(b_i) \tag{11}$$

The larger F' means the higher relation of the performance of the heat exchanger with evaluation grade j. The evaluation grade is obtained according to the maximum F'. Similarly, the correlated function and evaluation grade of the n-dimensional second-level matter element model could be deduced in the same way. When the different heat exchangers are placed at the same grade, characteristic value j^* is calculated to distinguish the discrepancy. The larger j^*, the higher performance of the heat exchanger.

$$j^* = \frac{\sum_{j=1}^{p} j\overline{F_j(T)}}{\sum_{j=1}^{p} \overline{F_j(T)}} \tag{12}$$

$$\overline{F_j(T)} = \frac{F_j(T) - F_j(T)_{\min}}{F_j(T)_{\max} - F_j(T)_{\min}} \tag{13}$$

3. Case study

In this study, in order to comprehensively evaluate the performance of the heat exchanger and then provide suggestions for the engineering application, the STHE and PCHE are chosen as the IHE with LBE and helium for comparison. The operating condition is shown in Table 2.

The whole STHE is made of 316L stainless steel and the counter-flow pattern is adopted shown in Figs. 1 and 2. Helium flows in the

Table 2
Operating condition.

Parameters	LBE	Helium
Inlet mass flow rate, kg/h	6735	133
Inlet temperature, °C	500	300
Outlet temperature, °C	350	450
Inlet pressure, MPa	0.5	3.0
Pressure drop, Pa	95	60
Heat transfer rate, kW	28.86	

shell and LBE in the tube. The outside diameter of the shell is 219 mm and the thickness of the shell is 6 mm. In order disturb the helium flow for increasing the heat transfer performance, eight segmental baffles are employed in the shell and four space rods are adopted to fix the distance between two baffles. The height and the spacing of the baffle is 141.1 mm and 217 mm, respectively. For the tube side, fifty-seven tubes are employed for the LBE flow, which are in a triangular cross arrangement. Therefore, the transverse and diagonal pitches are the same. The detail structural parameters of the STHE are presented in Table 3 [21].

In order to reach high performance, the counter-flow pattern is also adopted for the PCHE shown in Figs. 3 and 4. Single banking is chosen in which each of hot plates is followed by one of cold plates and the plate thickness is 1.5 mm. The number of the plates for each side of the PCHE is 60. The straight and semi-circle cross-sectional channel is manufactured on the 316L stainless steel plates to reduce the pressure drop. Due to the thermal resistances on the hot and cold sides are almost at the same order, the same channel structure is chosen for two sides. The channel diameter and pitch for each side of the PCHE are 1.6 mm and 2.0 mm, respectively. All the plates are welded together to form the heat exchanger and the cover plates are employed on the top and bottom of the welded plates to increase the structure strength. The dimensions of the core body of the PCHE are 310mm × 200 mm × 600 mm. The detail geometry parameters are summarized in Table 4.

In China, the levels of the students are divided into four grades according to the exam scores. These four grades are excellent, good, medium and poor, and the corresponding classical domains are [90, 100), [80, 90), [70, 80) and [60, 70). Therefore, the joint domain is [60, 100). This evaluation method is also adopted by Liu et al. [34] and is proved to be useful and reasonable. Therefore, in the study, this method is employed for assess the index in the comprehensive evaluation system of the heat exchanger. As shown in Table 5, the value range of the indexes corresponding to the score range [60, 100) are presented.

The comprehensive evaluation of the STHE and the PCHE is conducted, and the score of each index is shown in Table 6. The heat transfer areas are calculated based on the hot side of the heat exchanger. Detailed structural parameters for two heat exchangers are shown in Tables 3 and 4 The larger the heat transfer area, the higher heat transfer rate. In addition, the volume and mass could also be calculated based on the data in Tables 3 and 4

The logarithmic mean temperature differences are calculated according to the requirement of the ADS. For these two heat exchangers, the value is 50 based on the inlet and outlet temperatures in Table 2. The total heat transfer coefficient k is calculated based on the hot side of the heat exchanger as the index value by using the following equations.

$$k = \frac{1}{\frac{1}{h_o}\frac{A_i}{A_o} + R_w + \frac{1}{h_i}} \tag{14}$$

$$h = \frac{Nu\lambda}{D} \tag{15}$$

in which, h is the heat transfer coefficient on hot or cold side of the heat exchanger, W/(m^2·K). A is the heat transfer area on hot or cold side of the heat exchanger, m^2. R_w is the thermal resistance, (m^2·K)/W.

For the helium flow, the Nusselt number Nu is calculated as follows:

$$Nu = \frac{(f/8)(Re-1000)Pr}{1 + 12.7\sqrt{f/8}(Pr^{2/3}-1)} \tag{16}$$

$$f = (1.82 \lg Re - 1.64)^{-2} \tag{17}$$

in which, f is the friction factor on hot or cold side of the heat exchanger. Re is the Reynolds number and Pr is the Prandtl number. For the LBE flow, the Nusselt number Nu is calculated as follows [5]:

$$Nu = E + 0.018Pe^{0.8} \tag{18}$$

$$Pe = Re \times Pr \tag{19}$$

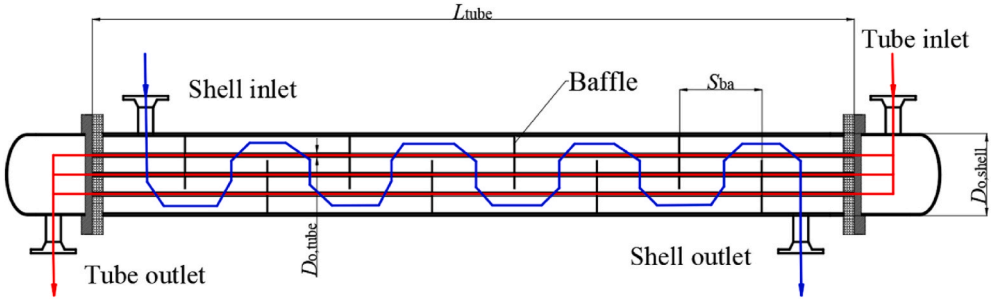

Fig. 1. Geometry of the STHE

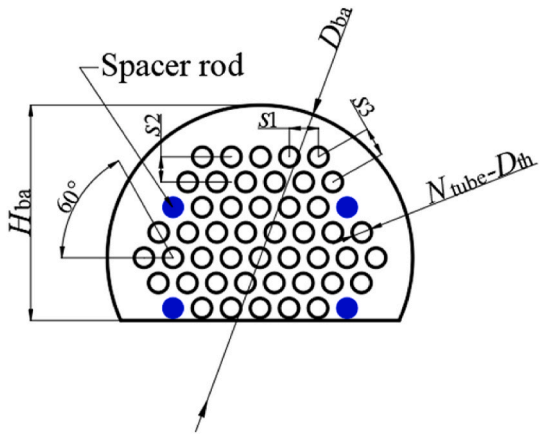

Fig. 2. Geometry of the baffle.

Table 3
Structural parameters of STHE.

Parameter	Value
Shell side	
Outside diameter of shell $D_{o,\ shell}$, mm	219
Inside diameter of shell $D_{i,\ shell}$, mm	207
Tube side	
limited circular diameter of tube arrangement D_{ta}, mm	164
Outside diameter of tube $D_{o,\ tube}$, mm	12
Inside diameter of tube $D_{i,\ tube}$, mm	9
Effective length of heat transfer L_{el}, mm	1942
Length of tube L_{tube}, mm	2000
Number of tube N_{tube}	57
Number of tube row N_{row}	9
Transverse pitch s_1, mm	19
Ratio of transverse pitch and outside diameter of tube α	1.58
Longitudinal pitch s_2, mm	16.45
Ratio of longitudinal pitch and outside diameter of tube β	1.37
Diagonal pitch s_3, mm	19
Ratio of diagonal pitch and outside diameter of tube γ	1.58
Segmental baffle	
Diameter of segmental baffle D_{ba}, mm	200
Diameter of tube hole D_{th}, mm	12.7
Height of baffle H_{ba}, mm	141.1
Thickness of baffle B_{ba}, mm	3
Number of baffle N_{ba}	8
Spacing of baffle S_{ba}, mm	217

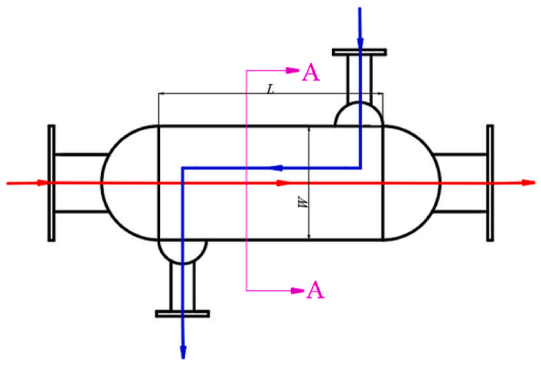

Fig. 3. Flow configuration of the PCHE.

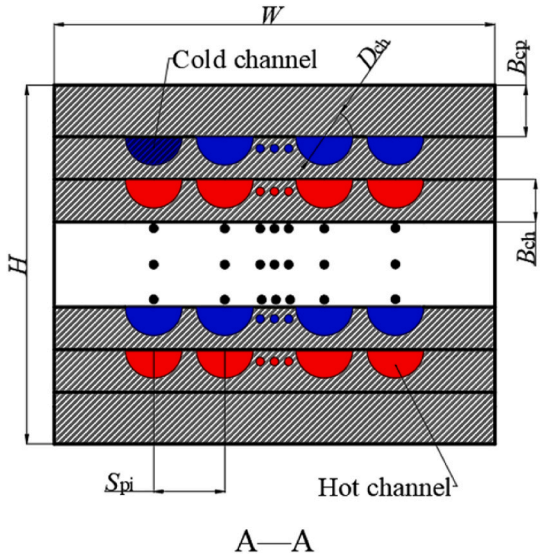

Fig. 4. Channel configuration of the PCHE.

Table 4
Structural parameters of PCHE.

Parameter	Cold side	Hot side
Channel diameter D_{ch}, mm	1.6	1.6
Thickness of channel plate B_{ch}, mm	1.5	1.5
Channel pitch S_{pi}, mm	2.0	2.0
Number of plate N_{pl}	60	60
Thickness of cover plate B_{cp}, mm	10	
Width of the PCHE W_{PCHE}, mm	310	
Height of the PCHE H_{PCHE}, mm	200	
Length of the PCHE L_{PCHE}, mm	600	

Table 5
Value and score ranges of indexes.

Index	Value	Score
Heat transfer areas, m^2	[3.20, 6.67)	[60, 100)
The logarithmic mean temperature differences, °C	[29.00, 69.00)	[60, 100)
Total heat transfer coefficient, W/(m^2·K)	[7.75, 194.89)	[60, 100)
Flow velocity on the hot side, m/s	[0.19, 0.00)	[60, 100)
Flow velocity on the cold side, m/s	[4.00, 0.00)	[60, 100)
Pressure loss on the hot side, Pa	[409.12, 0.00)	[60, 100)
Pressure loss on the cold side, Pa	[593.42, 0.00)	[60, 100)
Allowance stress, MPa	[17.00, 117.00)	[60, 100)
Design pressure, MPa	[2.60, 10.60)	[60, 100)
Weld joint factor	[1.43, 0.50)	[60, 100)
Lost circulation resistance	[0.60, 1.00)	[60, 100)
Corrosion resistance	[0.14, 1.92)	[60, 100)
Anti-fouling	[0.00, 11.64)	[60, 100)
Manufacture and installation cost, CNY	[215000.00,0.00)	[60, 100)
Depreciation cost, CNY	[10245.45, 0.00)	[60, 100)
Maintenance cost, CNY	[11880.95, 0.00)	[60, 100)
Volume, m^3	[0.10, 0.00)	[60, 100)
Mass, kg	[595.00, 0.00)	[60, 100)
Design cycle, day	[4.00, 0.00)	[60, 100)
Processing cycle, day	[83.57, 0.00)	[60, 100)

$$E = \begin{cases} 4.5 & Pe \leq 1000 \\ 5.4 - 9 \times 10^{-4}\, Pe & 1000 \leq Pe \leq 2000 \\ 3.6 & Pe \geq 2000 \end{cases} \tag{20}$$

Table 6
Scores of indexes for STHE and PCHE.

Index	STHE		PCHE	
	Value	Score	Value	Score
Heat transfer areas, m^2	4.16	71	5.46	86
The logarithmic mean temperature differences, °C	50	81	50	81
Total heat transfer coefficient, W/(m^2·K)	138.75	88	106	81
Flow velocity on the hot side, m/s	0.036	93	0.017	97
Flow velocity on the cold side, m/s	1.13	89	1.61	84
Pressure loss on the hot side, Pa	49.69	95	214	79
Pressure loss on the cold side, Pa	30.1	98	460	69
Allowance stress, MPa	107	96	107	96
Design pressure, MPa	4	67	10	97
Weld joint factor	0.85	85	0.92	82
Lost circulation resistance	0.85	85	0.95	95
Corrosion resistance	1.5	91	0.7	74
Anti-fouling	9	91	0.8	63
Manufacture and installation cost, CNY	45000	91	100000	81
Depreciation cost, CNY	2100	92	4900	81
Maintenance cost, CNY	300	98	6700	77
Volume, m^3	0.081	68	0.037	85
Mass, kg	340	77	220	85
Design cycle, day	3	71	2	81
Processing cycle, day	30	85	60	71

The total heat transfer coefficients for the STHE and PCHE are 138.75 W/(m^2·K) and 106 W/(m^2·K), respectively. The flow velocity V on both sides of the heat exchangers are calculated by the following equation:

$$V = \frac{q_m}{\rho A} \tag{21}$$

The pressure drops Δp on both sides of the heat exchangers are calculated by the following equation:

$$\Delta p = \frac{4fL\rho V^2}{D} \tag{22}$$

The allowance stress and design pressure of the heat exchangers are obtained from the National Standard of the People's Republic of China (GB150-2011). Corrosion resistance of the heat exchanger is obtained according to the thinnest part of the heat transfer tube or plate. For example, the thickness of the tube for the STHE is 1.5 mm and therefore the index value of corrosion resistance is 1.5. The larger index value, the better the corrosion resistance capability. For different heat exchangers, the anti-fouling is decided by the smallest channel dimension. Therefore, the small dimension in the flow channel is employed as the index value of the anti-fouling. Some of the index values, such as weld joint factor, lost circulation resistance, manufacture and installation cost, design and processing cycles, could be obtained from the processing factory. The depreciation cost could be obtained by using the straight-line method and after 20 years the residual values of the STHE and PCHE C_{rv} are 3000 CNY and 2000 CNY, respectively. Therefore, the depreciation cost C_{dc} per year could be calculated by the following equations:

$$C_{dc} = \frac{C_M - C_{rv}}{n} \tag{23}$$

in which, n is the life of the heat exchanger, y. C_M is the manufacture and installation cost, CNY.

The maintenance cost C_o could be obtained by the following equations:

$$C_o = C_E \sum_{i=1}^{2} W_{pi} \tag{24}$$

$$W_{pi} = \Delta p \frac{q_m}{\rho} \tag{25}$$

in which, C_E is the electrical price in China, CNY/(kW·h). W_{pi} is the pump power, W.

As a kind of compact heat exchanger, the PCHE has higher heat transfer area than that of the STHE, but lower heat transfer coefficient due to the lower Reynolds number. The average temperature difference is the same for two heat exchangers because the inlet and outlet temperatures are kept the same. Besides, the PCHE owns larger cross-sectional area and therefore the velocities on both sides are lower than those in the STHE. However, the pressure drops in the PCHE is higher due to the higher ratio of channel length to hydraulic diameter. Compared with the STHE, mini-channels formed on the plates in the PCHE could improve the design pressure, and the vacuum diffusion bonding, which owns higher weld joint factor and lower lost circulation resistance, is adopted to weld all the plates. The STHE has larger tube diameter and tube pitch, and therefore owns higher anti-fouling performance. The thicknesses of the tube and the shell for the STHE presents more advantage in corrosion resistance compared with the PCHE. Although the PCHE is

compact and lightweight, the STHE shows the lower cost due to the mature manufacture process. In addition, the manufacture processing cycle of the STHE is shorter than that of the PCHE. In conclusion, each heat exchanger has its own advantages and drawbacks.

The correlated functions of the index layers for the STHE and the PCHE are calculated shown in Tables 7 and 8.

The correlated functions of the criterion layers for the STHE and the PCHE are calculated shown in Tables 9 and 10.

From the above tables, it can be concluded that heat transfer, economy and safety and reliability performances have more effect on the evaluation result of heat exchangers. The evaluation grades of most parameters in the criterion layer for the STHE are good or excellent, except the structural performance. For the PCHE, it is noteworthy that the evaluation grades of safety and reliability performance is poor because the smaller channel diameter is easily clogged. Furthermore, the mini-channels manufactured on the thin plate would reduce the plate thickness and therefore decrease the level of the corrosion resistance. The grade of the production cycle for the PCHE is medium due to the immature processing technology in China.

Considering the effect of all the performance parameters, both the comprehensive evaluation grades for the STHE and the PCHE are good shown in Table 11. Therefore, the characteristic values for two heat exchangers are calculated further. As shown in Table 12, the results demonstrate that the comprehensive performance the PCHE is theoretically higher compared with the STHE because the characteristic value of the PCHE is larger than that of the STHE.

4. Conclusions

In this study, through the analysis on matter element model, a comprehensive evaluation system of heat exchangers is built. The classical and joint domains are confirmed according to the databases and expert opinion. The weights of the performance indexes of the heat exchanger are set based on fuzzy analytic hierarchy process. The correlated function and evaluation grade are defined. At last, a comprehensive evaluation method of heat exchangers based on extension theory is proposed.

The SHTE and PCHE are chosen as the IHE with LBE and helium of the ADS for theoretical comparison. Although the flow channel in the SHTE is larger and that in the PCHE, the pressure drop performance for these two heat exchangers show the same grade. This is because the cross-sectional area of the PCHE is large and therefore the fluid flow velocity is low. The mechanism performance of the PCHE attains the highest grade because the plates are welded by the vacuum diffusion bonding. In conclusion, these two heat exchangers show the same evaluation grade. However, the comprehensive performance of the PCHE is theoretically better than that of the STHE due to the larger characteristic value. With the develop of the processing technology and the wide application of the PCHE, the production cycle is shortened and the manufacture and cost is deduced. In the future, the comprehensive performance of the PCHE would be even better.

The method used in these two heat exchangers is also suitable for other heat exchangers. For the actual applications, the parameters in the criterion and index layers and the weights could be adjusted according to the designers' experience, actual conditions of producing process, and operating conditions.

Declaration of competing interest

We declare that no conflict of interest exists in the submission of this manuscript, and manuscript is approved by all authors for publication.

Table 7
Correlated functions of the index layer for the STHE.

Index	$F_1(b_i)$	$F_2(b_i)$	$F_3(b_i)$	$F_4(b_i)$	Weight
Heat transfer areas	−0.0833	0.1	−0.45	−0.6333	0.32
Average temperature difference	−0.3667	−0.05	0.1	−0.3214	0.22
Total heat transfer coefficient	−0.6	−0.4	0.2	−0.1429	0.46
Flow velocity on the hot side	−0.7667	−0.65	−0.3	0.3	0.3
Flow velocity on the cold side	−0.6333	−0.45	0.1	−0.0833	0.2
Pressure loss on the hot side	−0.8333	−0.75	−0.5	0.5	0.3
Pressure loss on the cold side	−0.9333	−0.9	−0.8	0.2	0.2
Allowance stress	−0.8667	−0.8	−0.6	0.4	0.3
Design pressure	−0.2917	0.3	−0.15	−0.4333	0.34
Weld joint factor	−0.5	−0.25	0.5	−0.25	0.36
Lost circulation resistance	−0.5	−0.25	0.5	−0.25	0.36
Corrosion resistance	−0.7	−0.55	−0.1	0.1	0.30
Anticorrosion	−0.7	−0.55	−0.1	0.1	0.34
Manufacture and installation cost	−0.7	−0.55	−0.1	0.1	0.38
Depreciation cost	−0.7333	−0.6	−0.2	0.2	0.30
Maintenance cost	−0.9333	−0.9	−0.8	0.2	0.32
Volume	0.2	−0.2	−0.6	−0.7333	0.58
Mass	−0.2917	0.3	−0.15	−0.4333	0.42
Design cycle	−0.0833	0.1	−0.45	−0.6333	0.42
Processing cycle	−0.5	−0.25	0.5	−0.25	0.58

Table 8
Correlated functions of the index layer for the PCHE.

Index	$F_1(b_i)$	$F_2(b_i)$	$F_3(b_i)$	$F_4(b_i)$	Weight
Heat transfer areas	−0.5333	−0.3	0.4	−0.2222	0.32
Average temperature difference	−0.3667	−0.05	0.1	−0.3214	0.22
Total heat transfer coefficient	−0.3667	−0.05	0.1	−0.3214	0.46
Flow velocity on the hot side	−0.9	−0.85	−0.7	0.3	0.3
Flow velocity on the cold side	−0.6	−0.4	0.2	−0.1429	0.2
Pressure loss on the hot side	−0.3214	0.1	−0.05	−0.3667	0.3
Pressure loss on the cold side	0.1	−0.1	−0.55	−0.7	0.2
Allowance stress	−0.8667	−0.8	−0.6	0.4	0.3
Design pressure	−0.9	−0.85	−0.7	0.3	0.34
Weld joint factor	−0.4	−0.1	0.2	−0.3077	0.36
Lost circulation resistance	−0.8333	−0.75	−0.5	0.5	0.36
Corrosion resistance	−0.2222	0.4	−0.3	−0.5333	0.30
Anticorrosion	0.3	−0.7	−0.85	−0.9	0.34
Manufacture and installation cost	−0.3667	−0.05	0.1	−0.3214	0.38
Depreciation cost	−0.3667	−0.05	0.1	−0.3214	0.30
Maintenance cost	−0.2917	0.3	−0.15	−0.4333	0.32
Volume	−0.5	−0.25	0.5	−0.25	0.58
Mass	−0.5	−0.25	0.5	−0.25	0.42
Design cycle	−0.3667	−0.05	0.1	−0.3214	0.42
Processing cycle	−0.0833	0.1	−0.45	−0.6333	0.58

Table 9
Correlated functions of the criterion layer for the STHE.

Criterion	$F_1(b_i)$	$F_2(b_i)$	$F_3(b_i)$	$F_4(b_i)$	j	Weight
Heat transfer	−0.3833	−0.163	−0.03	−0.339	3	0.19
Pressure drop	−0.7933	−0.69	−0.38	0.2633	4	0.12
Mechanism	−0.5392	−0.228	−0.051	−0.1173	3	0.11
Safety and reliability	−0.628	−0.442	0.116	−0.026	3	0.17
Economy	−0.7846	−0.677	−0.354	0.162	4	0.19
Structure	−0.0065	0.01	−0.411	−0.6073	2	0.10
Production cycle	−0.3249	−0.103	0.101	−0.41	3	0.12

Table 10
Correlated functions of the criterion layer for the PCHE.

Criterion	$F_1(b_i)$	$F_2(b_i)$	$F_3(b_i)$	$F_4(b_i)$	j	Weight
Heat transfer	−0.42	−0.13	0.196	−0.2897	3	0.19
Pressure drop	−0.4664	−0.325	−0.295	−0.1886	4	0.12
Mechanism	−0.1899	−0.565	−0.346	0.1112	4	0.11
Safety and reliability	−0.2646	−0.388	−0.559	−0.286	1	0.17
Economy	−0.3427	0.062	0.02	−0.3572	3	0.19
Structure	−0.5	−0.25	0.5	−0.25	3	0.10
Production cycle	−0.2023	0.037	−0.219	−0.5023	2	0.12

Table 11
Evaluation grade.

Case	$F_1(b_i)$	$F_2(b_i)$	$F_3(b_i)$	$F_4(b_i)$	j
STHE	−0.4814	−0.442	−0.043	−0.0832	3
PCHE	−0.341	−0.2649	−0.1037	−0.7092	3

Table 12
Characteristic value.

Case	j^*	Rank
STHE	3.41	2
PCHE	8.38	1

Data availability

Data will be made available on request.

Acknowledgements

This work is financially supported by the National Science and Technology Major Program of China (J2019-III-0021-0065).

References

[1] Y. Zhang, C. Wang, R. Cai, et al., Experimental investigation on flow and heat transfer characteristics of lead-bismuth eutectic in circular tubes, Appl. Therm. Eng. 180 (2020), 115820.
[2] X. Liu, D. Yang, Y. Yang, et al., Computational fluid dynamics and subchannel analysis of lead-bismuth eutectic-cooled fuel assembly under various blockage conditions, Appl. Therm. Eng. 164 (2020), 114419.
[3] Y. Wang, W. Xi, X. Li, et al., Influence of buoyancy on turbulent mixed convection of LBE in a uniform cooled inclined tube, Appl. Therm. Eng. 127 (2017) 846–856.
[4] Y. Shen, S. Peng, M. Yan, et al., Analytical study of heat transfer for liquid metals in a turbulent tube flow, Nucl. Eng. Des. 373 (2021), 111030.
[5] X. Cheng, N. Tak, Investigation on turbulent heat transfer to lead-bismuth eutectic flows in circular tubes for nuclear applications, Nucl. Eng. Des. 236 (2006) 385–393.
[6] S. He, M. Wang, J. Zhang, et al., Numerical simulation of three-dimensional flow and heat transfer characteristics of liquid lead-bismuth, Nucl. Eng. Technol. 53 (2021) 1834–1845.
[7] W. Ma, A. Karbojian, B.R. Sehgal, et al., Thermal-hydraulic performance of heavy liquid metal in straight-tube and U-tube heat exchangers, Nucl. Eng. Des. 239 (2009) 1323–1330.
[8] W. Xi, Y. Wang, X. Li, et al., Experimental investigation of the thermal hydraulics in lead bismuth eutectic-helium experimental loop of an accelerator-driven system, Nucl. Eng. Technol. 48 (2016) 1154–1161.
[9] F. Chen, J. Cai, X. Li, et al., 3D numerical simulation of fluid-solid coupled heat transfer with variable property in a LBE-helium heat exchanger, Nucl. Eng. Des. 274 (2014) 66–76.
[10] Y. Wang, H. Zhang, X. Huai, et al., Exergy analysis of LBE-helium heat exchanger in the experimental cooling loop based on accelerator driven sub-critical power system, Energy Convers. Manag. 135 (2017) 274–280.
[11] M.S. Khan, Y. Bai, Z. Chen, et al., Conceptual design and numerical assessment of compact heat exchanger for lead-based reactor, Prog. Nucl. Energy 124 (2020), 103348.
[12] J. Zhao, L. Li, W. Xie, et al., Flow and heat transfer characteristics of liquid metal and supercritical CO_2 in a twisted tube heat exchanger, Int. J. Therm. Sci. 174 (2022), 107453.
[13] Y. Yang, C. Wang, D. Zhang, et al., Numerical analysis of liquid metal helical coil once-through tube steam generator, Ann. Nucl. Energy 167 (2022), 108860.
[14] H. Zhang, K. Cheng, X. Huai, et al., Experimental and numerical study of an 80-kW zigzag printed circuit heat exchanger for supercritical CO_2 Brayton cycle, J. Therm. Sci. 30 (4) (2021) 1289–1301.
[15] S. Liu, R. Liu, Y. Huang, et al., Experimental study on flow and heat transfer of supercritical carbon dioxide in zigzag channels with bending angle 30° for advanced nuclear systems, Ann. Nucl. Energy 185 (2023), 109720.
[16] H. Zhang, L. Shi, W. Xuan, et al., Analysis of printed circuit heat exchanger potential in exhaust waste heat recovery, Appl. Therm. Eng. 204 (2020), 117863.
[17] Y. Yang, H. Li, B. Xie, et al., Experimental study of the flow and heat transfer performance of a PCHE with rhombic fin channels, Energy Convers. Manag. 254 (2022), 115137.
[18] J. Zhou, K. Cheng, H. Zhang, et al., Test platform and experimental test on 100 kW class printed circuit heat exchanger for supercritical CO_2 Brayton cycle, Int. J. Heat Mass Tran. 140 (2020), 118540.
[19] J. Wang, Y. Ma, T. Ma, et al., Design and thermal-hydraulic analysis of a printed circuit heat exchanger for ADS applications, Energy 256 (2022), 124598.
[20] P. Xu, T. Zhou, Z. Fu, et al., Heat transfer performance of liquid lead-bismuth eutectic and supercritical carbon dioxide in double D-type straight channel, Appl. Therm. Eng. 219 (2023), 119484.
[21] Y. Wang, X. Li, X. Huai, et al., Experimental investigation of a LBE-helium heat exchanger based the ADS, Prog. Nucl. Energy 99 (2017) 11–18.
[22] D. Zhang, H. Zhang, Q. Wang, et al., Effect of heat flux distribution on entropy generation and irreversibility of lead-bismuth eutectic forced convective heat transfer, J. Therm. Sci. 32 (1) (2023) 223–236.
[23] A.B. Krishna, K. Jin, P.S. Ayyaswamy, et al., Technoeconomic optimization of superalloy supercritical CO2 microtube shell-and-tube-heat exchangers, Appl. Therm. Eng. 220 (2022), 119578.
[24] M. Asadi, Y. Song, B. Sunden, et al., Economic optimization design of shell-and-tube heat exchangers by a cuckoo-search-algorithm, Appl. Therm. Eng. 73 (1) (2015) 1032–1040.
[25] I.H. Kim, X. Zhang, R. Chistensen, et al., Design study and cost assessment of straight, zigzag, S-shape, and OSF PCHEs for a FLiNaK-SCO_2 secondary heat exchangers in FHRs, Ann. Nucl. Energy 94 (2016) 129–137.
[26] J.F. Hinze, G.F. Nellis, M.H. Anderson, Cost comparison of printed circuit heat exchanger to low cost periodic flow regenerator for use as recuperator in a s-CO_2 Brayton cycle, Appl. Energy 208 (2017) 1150–1161.
[27] K. Bennett, Y. Chen, One-way coupled three-dimensional fluid-structure interaction analysis of zigzag-channel supercritical CO_2 printed circuit heat exchangers, Nucl. Eng. Des. 358 (2020), 110434.
[28] R. Torre, J. Francois, C. Lin, Assessment of the design effects on the structural performance of the printed circuit heat exchanger under very high temperature condition, Nucl. Eng. Des. 365 (2020), 110713.
[29] W. Cai, Extension theory and its application, Chin. Sci. Bull. 44 (1999) 1538–1548.
[30] C. Qiao, Y. Wang, C. Li, et al., Application of extension theory based on improved entropy weight method to rock slope analysis in cold regions, Geotech. Geol. Eng. 39 (2021) 4315–4327.
[31] Y. Dong, Q. Peng, R. Tan, et al., Product function redesign based on extension theory, Computer-Aided Desig. Appl. 18 (1) (2020) 199–210.
[32] W. Wang, H. Wang, B. Zhang, et al., Coal and gas outburst prediction model based on extension theory and its application, Progress Safet. Environ. Protect. 154 (2021) 329–337.
[33] X. Bian, H. Pan, K. Zhang, et al., Skin lesion image classification method based on extension theory and deep learning, Multimed. Tool. Appl. 81 (2022) 16389–16409.
[34] J. Liu, H. Cui, X. Dai, et al., Multilevel comprehensive evaluation for heat exchanger design schemes based on extension theory, CIESC J. 62 (7) (2011) 1970–1976.
[35] D. Liu, S. Yang, An Information System Security Risk Assessment Model Based on Fuzzy Analytic Hierarchy Process, International Conference on E-Business and Information System Security, Wuhan China, 2009, pp. 1–4, 2009.

Nomenclature

A_i: Heat transfer area on inside channel, m^2

A_o: Heat transfer area on outside channel, m^2
a_{hk}: The *hk* index in the second-level model
a_i: The *i* criterion in the first-level model
B_{ba}: Thickness of baffle, mm
B_{ch}: Thickness of channel plate, mm
B_{cp}: Thickness of cover plate, mm
b_{hk}: The *hk* value in the second-level model
b_i: The *i* value in the first-level model
C_E: The electrical price in China, CNY/(kW·h)
C_{dc}: The depreciation cost, CNY
C_M: The manufacture and installation cost, CNY
C_o: The maintenance cost, CNY
C_{rv}: The residual values, CNY
D: Hydraulic diameter, mm
D_{ba}: Diameter of segmental baffle, mm
D_{ch}: Channel diameter, mm
$D_{i,tube}$: Inside diameter of tube, mm
$D_{i,shell}$: Inside diameter of shell, mm
$D_{o,shell}$: Outside diameter of shell, mm
$D_{o,tube}$: Outside diameter of tube, mm
D_{ta}: Limited circular diameter of tube arrangement, mm
D_{th}: Diameter of tube hole, mm
F': The relation of comprehensive evaluation with the evaluation grade
f: Friction factor
F_j: The correlated function of the first-level matter element model relating to evaluation grade *j*
H_{ba}: Height of baffle, mm
H_{PCHE}: Height of the PCHE, mm
h_i: heat transfer coefficient on inside channel, $W/(m^2 \cdot K)$
h_o: heat transfer coefficient on outside channel, $W/(m^2 \cdot K)$
j^*: Characteristic value
K: The location of point
k: The total heat transfer coefficient, $W/(m^2 \cdot K)$
L: Length, mm
L_{el}: Effective length of heat transfer, mm
L_{ttube}: Length of tube, mm
L_{PCHE}: Length of the PCHE, mm
N_{ba}: Number of baffle
N_{pl}: Number of plate
N_{row}: Number of tube row
N_{tube}: Number of tube
Δp: Pressure drop, Pa
Pe: Peclet number
Pr: Prandlt number
q_m: Mass flow rate, kg/s
Re: Reynolds number
R_{0ji}: Classical domain
R_{pi}: Joint domain
R_w: Thermal resistance, $(m^2 \cdot K) / W$
S_0: The first-level matter element model
S'_0: The second-level matter element model
s_1: Transverse pitch, mm
s_2: Longitudinal pitch, mm
s_3: Diagonal pitch, mm
S_{ba}: Spacing of baffle, mm
S_{pi}: Channel pitch, mm
S_p: The first-level matter element model relating to all the evaluation grades
T_0: Specific scheme in the target layer
T_{0h}: The criterion in the criterion layer
T_{0j}: Evaluation grade in the target layer
T_p: All the evaluation grades in the target layer
V: Velocity, m/s
w_{hk}: The weight of the parameter in the *hk* index layer
w_i: The weight of the parameter in the *i* criterion layer
W_{PCHE}: Width of the PCHE, mm
W_{pi}: Pump power, W
x_{0jm}: The bottom margin of the classical domain
x_{pi}: The bottom margin of the joint domain
y_{0jm}: The top margin of the classical domain
y_{pi}: The top margin of the joint domain

Greek letters

α: Ratio of transverse pitch and outside diameter of tube
β: Ratio of longitudinal pitch and outside diameter of tube
ρ: Density, kg/m^3
γ: Ratio of diagonal pitch and outside diameter of tube
λ: Thermal conductivity, W/(m·K)
ξ: The distance between the point and the domain

Subscripts

ba: Baffle
ch: Channel
cp: Cover plate
el: Effective length
ta: Tube arrangement
th: Tube hole
pl: plate
pi: Pitch